Spread Spectrum-Coded OFDM Chirp Waveform Diversity Design

Sheng-Juan Cheng, Wen-Qin Wang, *Member, IEEE*, and Huai-Zong Shao

***Abstract*— This paper proposes an approach to design multiple-input multiple-output radar waveforms that are orthogonal on both the transmitter and receiver. The proposed method jointly utilizes the direct sequence spread spectrum coding and orthogonal frequency division multiplexing (OFDM) chirp signaling techniques. We name it spread spectrum-coded OFDM chirp waveform diversity design. The performance of the designed waveforms is analyzed by examining the ambiguity function and correlation function. The influences of the spread spectrum code choice and the OFDM chirp parameters are also investigated. It is verified that the proposed design scheme can ensure these waveforms stay orthogonal on the receiver and have large time-bandwidth product which is beneficial to separate closely spaced targets.**

***Index Terms*— Waveform diversity, multiple-input multiple-output (MIMO) radar, orthogonal frequency division multiplexing (OFDM), direct sequence spread spectrum (DSSS), spread spectrum coded OFDM chirp (SSCOC), ambiguity function.**

I. Introduction

MULTIPLE-INPUT multiple-output (MIMO) radar employs multiple transmit and receive antennas equipped with the capability of transmitting arbitrary waveforms at each transmit antenna. The added flexibility of individual signal selection at each antenna brings with it the promise of enormous performance improvements and the challenge of finding solutions to extremely high-dimensional optimization problems associated with choosing the right signals. As a consequence, MIMO radar has gained great popularity and attracted much attention in recent years [1]–[4]. However, waveform diversity design still is the most important and challenging issue in realizing MIMO radar concept.

To address MIMO radar waveform diversity design issues, some methods such as employing polarization diverse waveform [5], phase coded waveform [6], and combination of these methods [7] are proposed. A polarization diverse waveform enabling weak target detection is proposed in [8] for MIMO radar. Gladkova [9] designed a family of stepped frequency waveforms to attain high range resolution. In fact, many existing methods are based on the assumption that the waveforms stay orthogonal at the receiver under any Doppler frequency shifts [10]. An approach is proposed in [11] to design the radar waveforms that are orthogonal on both transmitter and receiver. It incorporates the Walsh-Hadamard code and chirp signal to design two orthogonal waveforms. A novel orthogonal frequency division multiplexing (OFDM) chirp waveform design scheme is proposed in [12], but it generates only two orthogonal waveforms; Otherwise, it will generate grating lobes in the ambiguity function response.

To generate more orthogonal waveforms, this paper proposes a waveform diversity design scheme by jointly utilizing the OFDM chirp waveform [12] and spread spectrum sequence. The use of OFDM signal in radar systems was proposed in 2000 [13]. The primary disadvantage of using OFDM in wireless communication lies in that time and frequency synchronization is crucial to ensure subcarrier orthogonality; However, sensitivity to time and frequency synchronization is beneficial for radar systems because radar receiver usually uses a stored version of the transmit signal to measure the time-delay and frequency offset between the transmitted and received signals to derive the target parameters [14]–[16]. For these advantages, OFDM radar has received considerable attention in recent years [17], [18]. In this paper, we use a unique spread spectrum code to further modulate the OFDM chirp waveforms. In doing so, the transmitted waveforms can be successfully filtered only with the intended waveform. The uses of Walsh-Hadamard code, m-sequence, GOLD sequence and orthogonal GOLD sequence are comparatively investigated. The performance of the designed waveforms are analyzed by examining the ambiguity function and correlation function.

The remaining sections are organized as follows. Section II introduces the background and motivation of our work. Section III presents the spread spectrum coded OFDM chirp (SSCOC) waveform. Section IV discusses several design issues such as spread spectrum sequence choice and bandwidth reduction. Next, Section V analyzes the designed waveform performance. Finally, Section VI concludes the paper.

II. Background and Motivation

Chirp waveform can achieve constant envelope in both time domain and frequency domain and thus, a large

Manuscript received November 7, 2014; accepted June 19, 2015. Date of publication June 23, 2015; date of current version August 12, 2015. This work was supported in part by the National Natural Science Foundation of China under Grant 41101317, in part by the Program for New Century Excellent Talents in University under Grant NCET-12-0095, and in part by the Sichuan Province Science Fund for Distinguished Young Scholars under Grant 2013JQ0003. The associate editor coordinating the review of this paper and approving it for publication was Dr. M. Nurul Abedin.

S.-J. Cheng and H.-Z. Shao are with the School of Communication and Information Engineering, University of Electronic Science and Technology of China, Chengdu 611731, China (e-mail: shengjuancheng@gmail.com; hzshao@uestc.edu.cn).

W.-Q. Wang is with the School of Communication and Information Engineering, University of Electronic Science and Technology of China, Chengdu 611731, China, and also with the Department of Electrical and Electronic Engineering, Imperial College London, London SW7 2AZ, U.K. (e-mail: wqwang@uestc.edu.cn).

Color versions of one or more of the figures in this paper are available online at http://ieeexplore.ieee.org.

Digital Object Identifier 10.1109/JSEN.2015.2448617

time-bandwidth product can be obtained [20], [21]. The OFDM chirp waveform diversity design proposed in [12] is a promising technique, which exploits the orthogonality of the discrete frequency components. The design scheme has the following features: First, the OFDM chirp waveform has similar characteristics of chirp waveform. Second, the scheme has a high adaptability, which implies that the waveform design scheme can be easily combined with other waveform design schemes, such as the space-frequency coding or the multidimensional encoding technique. Note, however, that the method designs only two orthogonal waveforms. More seriously, the waveforms will be significantly degraded by the grating lobes. It is thus necessary to design more orthogonal waveforms and suppress the grating lobes. One potential solution is to further modulate the OFDM chirp waveform with spread spectrum sequences.

Spread spectrum technique is widely used in wireless communications. Typical spread spectrum sequences are the Walsh-Hadamard code, m sequence, GOLD sequence and orthogonal GOLD sequence. Suppose the information to be transmitted is

$$A(t) = \sum_{n=-\infty}^{+\infty} a_n P(t - nT_b) \tag{1}$$

where $a_n = \pm 1$, $P(t)$ is a rectangular function, and T_b is the pulse duration. Then, modulating $A(t)$ with a spread spectrum sequence

$$C(t) = \sum_{n=-\infty}^{+\infty} c_n P(t - nT_c) \tag{2}$$

yields

$$B(t) = A(t)C(t) \tag{3}$$

where c_n is binary pseudorandom (PN) code of ± 1 and T_c is the chip duration. Suppose the carrier frequency is f_c, the transmitted signal can then be expressed as

$$T_x(t) = A(t)C(t)\cos(2\pi f_c t). \tag{4}$$

Accordingly, the received signal is

$$R_x(t) = A(t)C(t)\cos(2\pi f_c t) + I(t) \tag{5}$$

where $I(t)$ is the additive noise. Demodulating $R_x(t)$ with $C(t)$ yields

$$D_x(t) = R_x(t)C(t) = \{A(t)C(t)\cos(2\pi f_c t) + I(t)\}\, C(t). \tag{6}$$

Therefore, the demodulated signal satisfies $D_x(t) = A(t)$.

III. Spread Spectrum Coded OFDM Chirp Waveform

As shown in Figure 1, suppose the elements in the input sequence $S[p]$ are separated by $2\Delta f$ in frequency domain, wherein $S_1[p]$ is obtained by interleaving $S[p]$ with $3N$ zeros. Accordingly, $S_2[p]$, $S_3[p]$ and $S_4[p]$ are generated by shifting $S_1[p]$ for $\Delta f/2$, Δf and $3\Delta f/2$, respectively. In doing so, we will have four waveforms modulated by four orthogonal subcarrier sets that are mutually shifted by $\Delta f/2$. It must be emphasized that all the sets contain $4N$ subcarriers but each uses only N subcarriers.

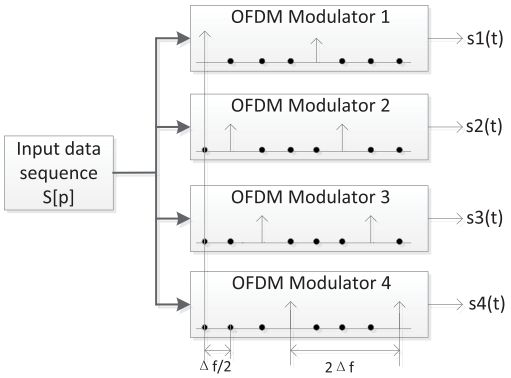

Fig. 1. Four orthogonal OFDM chirp waveforms generate scheme.

According to the design scheme, a chirp signal is used for the OFDM modulation to achieve a constant envelope. In practical implementation using digital devices, the discrete-time samples are denoted by

$$s[m] = \exp\left(j\pi k_r (mT_s)^2\right), \quad m = 0, 1, \ldots, N-1 \tag{7}$$

where T_s is the sampling interval and k_r is the chirp rate which is a ratio between the signal bandwidth B and chirp duration T_p, namely, $k_r = B/T_p$. After Fourier transform, we have

$$S[p] = \mathscr{F}\{s[m]\} = \mathscr{F}\left\{\exp\left(j\pi k_r (mT_s)^2\right)\right\} \tag{8}$$

where $\mathscr{F}\{\cdot\}$ is the Fourier transform operator. Using $S[p]$ as the input sequence, the time-domain waveform $s_1[n]$ can be expressed as

$$\begin{aligned} s_1[n] = \frac{1}{4}\Bigg\{ & s[n]\mathrm{rect}\left[\frac{n}{N}\right] + s[n-N]\mathrm{rect}\left[\frac{n-N}{N}\right] \\ & + s[n-2N]\mathrm{rect}\left[\frac{n-2N}{N}\right] \\ & + s[n-3N]\mathrm{rect}\left[\frac{n-3N}{N}\right]\Bigg\} \end{aligned} \tag{9}$$

where $n = 0, 1, \ldots, 4N-1$.

Supposing $\Delta f = 1/2NT_s$, since the four orthogonal subcarrier sets are mutually shifted by $\Delta f/2$, the other three waveforms can be derived directly from $s_1[n]$ as follows:

$$s_i[n] = s_1[n]\exp\left(j\frac{(i-1)\pi n}{2N}\right), \quad i = 2, 3, 4. \tag{10}$$

Their corresponding continuous-time representations are expressed, respectively, as

$$\begin{aligned} s_1(t) = \frac{1}{4}\Bigg\{ & s(t)\mathrm{rect}\left[\frac{t}{T_p}\right] + s(t-T_p)\mathrm{rect}\left[\frac{t-T_p}{T_p}\right] \\ & + s(t-2T_p)\mathrm{rect}\left[\frac{t-2T_p}{T_p}\right] \\ & + s(t-3T_p)\mathrm{rect}\left[\frac{t-3T_p}{T_p}\right]\Bigg\} \end{aligned} \tag{11}$$

$$s_i(t) = s_1(t)\exp\left(j\pi\frac{it}{4T_p}\right), \quad i = 2, 3, 4. \tag{12}$$

To suppress grating lobes in the OFDM chirp waveforms, we further use spread spectrum sequence to modulate them. For simplicity and without loss of generality, we take the OFDM chirp signal $s_1(t)$ and $s_2(t)$ as example waveforms to introduce the design scheme. They are represented, respectively, by

$$sc_1(t) = \sum_{m}^{M-1} C_m P(t - mT_c) s_1(t) \tag{13}$$

$$sc_2(t) = \sum_{n}^{M-1} D_n P(t - nT_c) s_2(t) \tag{14}$$

where C_m and D_n are the first and second code sequences, respectively.

To further investigate what happens when the targets are moving, we correlate the emitted pulse with a copy shifted in range and Doppler frequency shift. This performance can be evaluated by the cross-ambiguity function between $sc_1(t)$ and $sc_2(t)$ [19]

$$\begin{aligned}
&\chi_{sc_1,sc_2}(\tau, f_d) \\
&= \int_R sc_1(t) sc_2^*(t-\tau) \exp(j2\pi f_d t)\, \mathrm{d}t \\
&= \int_R \left(\sum_{m}^{M-1} C_m P(t - mT_c) s_1(t) \right) \\
&\quad \times \left(\sum_{n}^{M-1} D_n P(t - nT_c - \tau) s_2(t-\tau) \right)^* \exp(j2\pi f_d t)\, \mathrm{d}t \\
&= \sum_{m}^{M-1} \sum_{n}^{M-1} C_m D_n^* \int_R P(t - mT_c) s_1(t) P(t - nT_c - \tau) \\
&\quad \times s_2^*(t-\tau) \exp(j2\pi f_d t)\, \mathrm{d}t
\end{aligned} \tag{15}$$

where f_d is the Doppler frequency shift, τ is the delay time, and * is the complex conjugate operator. Specially, when $sc_1(t) = sc_2(t)$, it simplifies to the auto-ambiguity function. The ambiguity function evaluated at $(\tau, f_d) = (0, 0)$ is equal to the matched filtering output that is matched perfectly to the signal reflected from the target of interest.

According to (15), some important properties of the SSCOC waveforms can be summarized as following:

1) The choice of spread spectrum code will influence the ambiguity response.
2) The code length will determine the orthogonality performance of the received signal. Furthermore, the waveform bandwidth expansion will be impacted by the code length.
3) The pulse duration T_p and bandwidth B will influence the cross-ambiguity function.
4) When the code C_m and D_n are orthogonal, then $\chi_{s_1,s_2}(\tau, f_d) \cong 0$. This implies that their cross-ambiguity function will be almost zero if orthogonal C_m and D_n are used.
5) If $C_m = D_n$, (15) simplifies to the auto-ambiguity function $\chi_{s_1,s_1}(\tau, f_d)$.

All these properties will be further verified by simulation results in subsequent sections.

TABLE I
SIMULATION PARAMETERS OF OFDM CHIRP SIGNALS

Parameters	Values
Bandwidth (B)	4 MHz
Pulse duration (T_p)	1 μs
Chirp rate (K_r)	B/T_p
Code length	2^m or $2^m - 1$ (m=2, 3, 4, 5, 6, 7)

TABLE II
COMPARATIVE max $\{CAF\}$ IN DIFFERENT DSS CODE LENGTH

code type	code length	BW (MHz)	max $\{CAF\}$
-	1	4	0.9988
Walsh	4	20	0.7234
Walsh	8	36	0.6649
Walsh	16	68	0.5551
Walsh	32	132	0.4887
Walsh	64	260	0.4196
Walsh	128	516	0.3649

IV. SEVERAL DESIGN ISSUES

Using the parameters listed in Table I, we analyze the influence of spread spectrum code length NC, code type, original bandwidth B and pulse duration T_p on the cross-ambiguity function. Note that the cross-ambiguity response is normalized by the auto-ambiguity peak to compare their differences clearly.

A. Impact of Spread Spectrum Code Length

The SSCOC waveform bandwidth is determined by

$$\mathrm{BW} = B\left(\frac{1}{T_p} + \frac{1}{T_c}\right). \tag{16}$$

When $B = 4$ MHz, the BWs of 20 MHz, 36 MHz, 68 MHz, 132 MHz, 260 MHz and 516 MHz correspond to the code lengths of 4, 8, 16, 32, 64 and 128, respectively. Without loss of generality, Walsh-Hadamard code is used in all the simulations. Table II compares the maximal cross-ambiguity function (CAF), namely max {CAF}. Note that no spread spectrum codes are used in the first line. It can be noticed that, a longer spread spectrum code length means a lower CAF peak level and better waveform orthogonality performance.

B. Impact of Spread Spectrum Code Type

We consider several typical spread spectrum codes, namely, Walsh-Hadamard code, m sequence, Gold sequence and orthogonal GOLD sequence on the designed waveform performance. For Walsh-Hadamard code and orthogonal GOLD sequence, the code lengths are 2^l $(l = 2, 3, 4, 5, 6, 7)$, whereas the length of $2^l - 1$ is used for the m and Gold sequences. Figure 2 compares max $\{CAF\}$ when different code types are employed. It is noticed that, when the GOLD sequence is used, it has the best orthogonality performance. The observed max $\{CAF\}$ is about 0.2 when the code length is 127. Take both bandwidth and orthogonality into consideration, GOLD code is the best suitable code to be applied in the SSCOC signaling and orthogonal GOLD sequence is the second one. It can be estimated that if we want

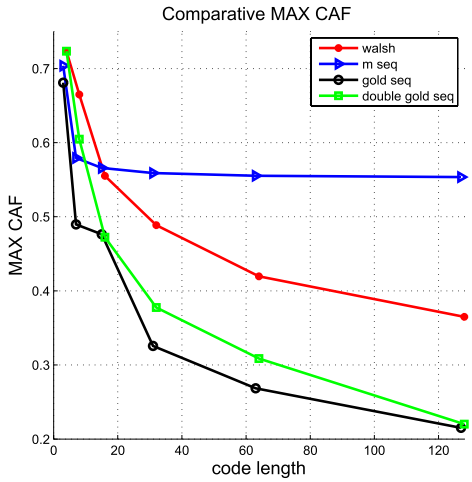

Fig. 2. Comparative max $\{CAF\}$ among different types.

TABLE III
BANDWIDTH REDUCTION COMPARISON WHEN $NC = 64$

code type	code length	BW (MHz)	max $\{CAF\}$
-	64	0.01	0.4196
Walsh	64	0.1	0.4196
Walsh	64	1	0.4259
Walsh	64	4	0.4196
Walsh	64	20	0.4196
Walsh	64	100	0.4196
Walsh	64	1000	0.4196

to obtain lower max $\{CAF\}$, a longer code length should be employed.

C. Bandwidth Reduction Property of SSCOC Signaling

From Table II, we can see that the bandwidth expansion will be greater for increased code length. In practical application, frequency spectra is a scarce resource. In particular, using bandwidth larger than 1 GHz could be expensive for hardware implementation. To analyze the bandwidth reduction problem, we consider the BWs of 0.01 MHz, 0.1 MHz, 1 MHz, 4 MHz, 20 MHz, 100 MHz and 1000 MHz, respectively. Supposing $T_p = 1\ \mu s$ and $NC = 64$, Table III shows that the initial bandwidth B has no influence on the max $\{CAF\}$. This is an important property of the SSCOC signaling and thus we can reduce the coded bandwidth by employing a small initial bandwidth.

D. Impact of Pulse Duration

High chirp rate demands high performance hardware device. Since the bandwidth almost has no influence on the CAF response, we can enlarge the duration T_p to reduce the chirp rate k_r. Table IV compares the impact of pulse duration on the max $\{CAF\}$. It is noticed that different pulse durations produce nearly an equivalent orthogonality performance. This property is useful to reduce the hardware design difficulty.

V. WAVEFORM PERFORMANCE ANALYSIS

In this section, we further compare the performance of the designed waveforms with conventional spread spectrum coded chirp (SSCL) waveform [11], DSSS-modulated two-OFDM scheme named as SSCTOC [12], and OFDM chirp waveforms mentioned in Section III, respectively.

TABLE IV
PULSE DURATION INFLUENCE ON THE CAF RESPONSE

code type	code length	pulse duration (μs)	max $\{CAF\}$
-	64	0.001	0.4196
Walsh	64	0.01	0.4196
Walsh	64	0.1	0.4196
Walsh	64	1	0.4196
Walsh	64	10	0.4196
Walsh	64	100	0.4256
Walsh	64	1000	0.4196

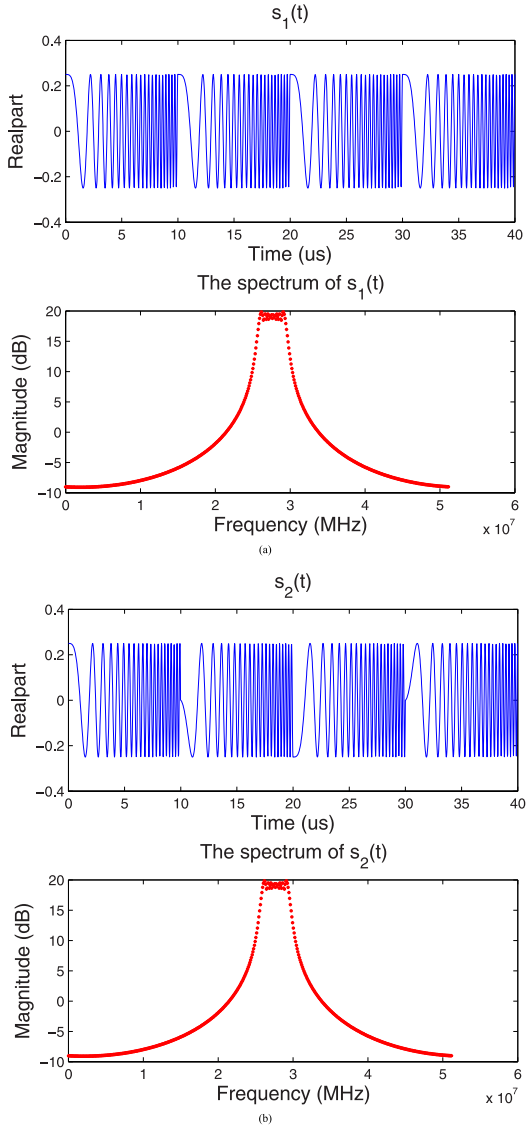

Fig. 3. Time-domain and frequency-domain of basic OFDM chirp waveform. (a) $s_1(t)$. (b) $s_2(t)$.

A. OFDM Chirp Waveforms and SSCOC Waveforms Comparison

For simplicity and without loss of generality, OFDM chirp waveforms $s_1(t)$, $s_2(t)$ and SSCOC waveforms

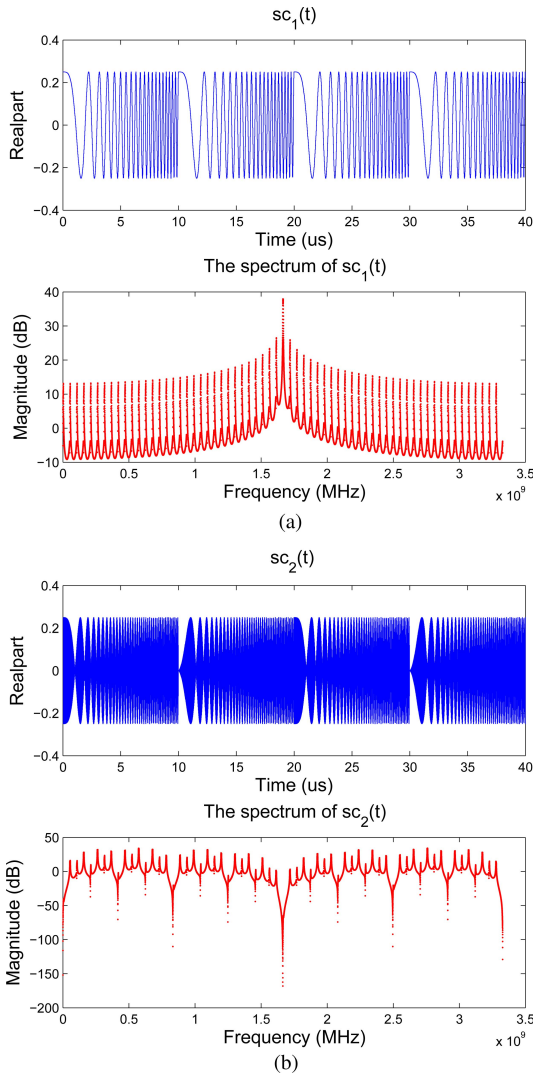

Fig. 4. Time-domain and frequency-domain of SSCOC waveform. (a) $sc_1(t)$. (b) $sc_2(t)$.

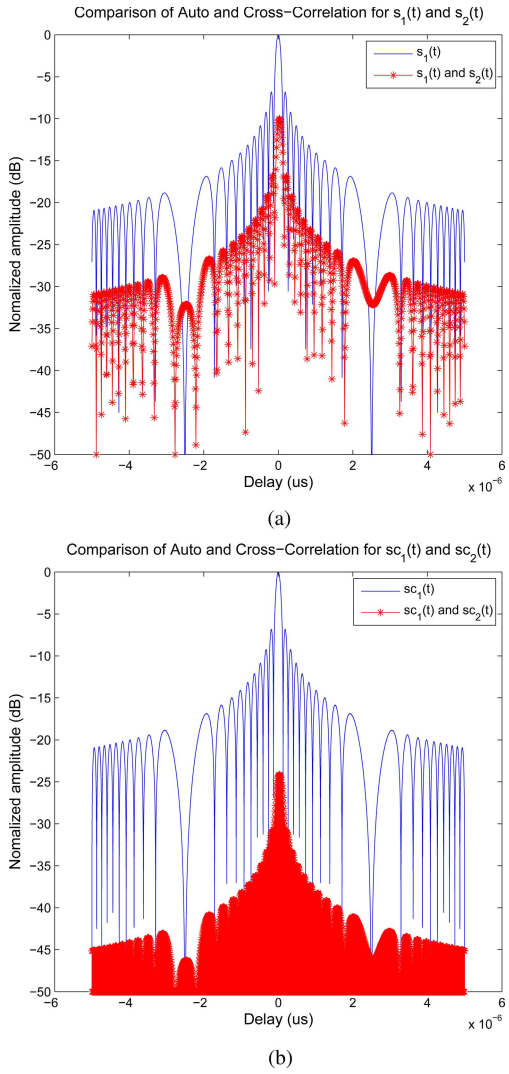

Fig. 5. Comparisons between waveform auto and cross-correlations. (a) Between $s_1(t)$ and $s_2(t)$. (b) Between $sc_1(t)$ and $sc_2(t)$.

$sc_1(t)$, $sc_2(t)$ are considered as an example to compare their performances.

1) Time-Domain and Frequency-Domain Comparisons: The simulation is carried out under the following assumptions: the input sequence length N is 512, so that the lengths of the OFDM chirp waveforms $s_1(t)$ and $s_2(t)$ are $4N$, namely, 2048. And the initial bandwidth is $B = 4$ MHz, and pulse duration is $T_p = 10\ \mu s$. The Walsh-Hadamard code with a length of 64 is used. According to (16), the corresponding bandwidth BW of $sc_1(t)$ and $sc_2(t)$ is 260 MHz.

It is clear from Figure 3 that $s_1(t)$ and $s_2(t)$ have an $\pi/2$ phase difference in the starting phases in time domain. They occupy the same frequency bandwidth and show the similar curves in frequency domain. However, the SSCOC waveforms $sc_1(t)$ and $sc_2(t)$ have no $\pi/2$ phase difference any more, as shown in Figure 4. Note that, due to different code sequences used in the simulations, $sc_2(t)$ has faster jump than $sc_1(t)$ in time domain and consequently their frequency-domain representations demonstrate obvious differences in both shape and magnitude.

2) Auto- and Cross-Correlation Analysis: The impacts of undesired waveform cross interferences on MIMO radar can be equivalently evaluated by the cross-correlation function, which is defined as

$$R_{xy}(\tau) = \int_{-\infty}^{+\infty} x(t)y^*(t-\tau)\mathrm{d}t. \tag{17}$$

When $x(t) = y(t)$, it simplifies to the auto-correlation function.

It can be noticed from Figure 5 that both design schemes provide good auto-correlation and cross-correlation performance. Compared with the basic OFDM chirp waveforms, the SSCOC waveforms have better cross-correlation suppression performance. Note that, if their returns are Doppler frequency shifted, this is also true because Doppler effect brings an equivalent frequency shift on them.

3) Auto- and Cross-Ambiguity Analysis: It is necessary to further use (15) to analyze the waveform auto-ambiguity and cross-ambiguity functions. Figure 6 compares the auto-ambiguity function of the waveforms $s_1(t)$ and $sc_1(t)$.

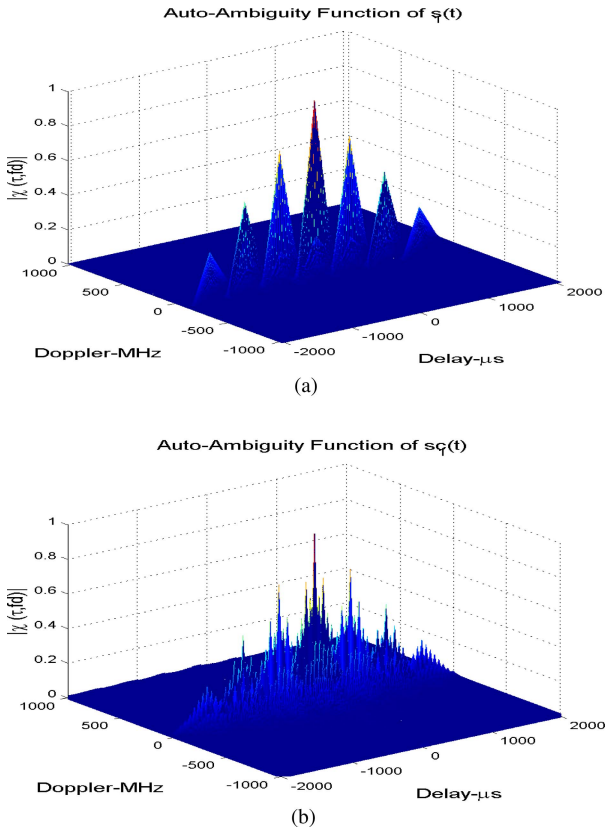

Fig. 6. Auto-ambiguity function results. (a) $s_1(t)$. (b) $sc_1(t)$.

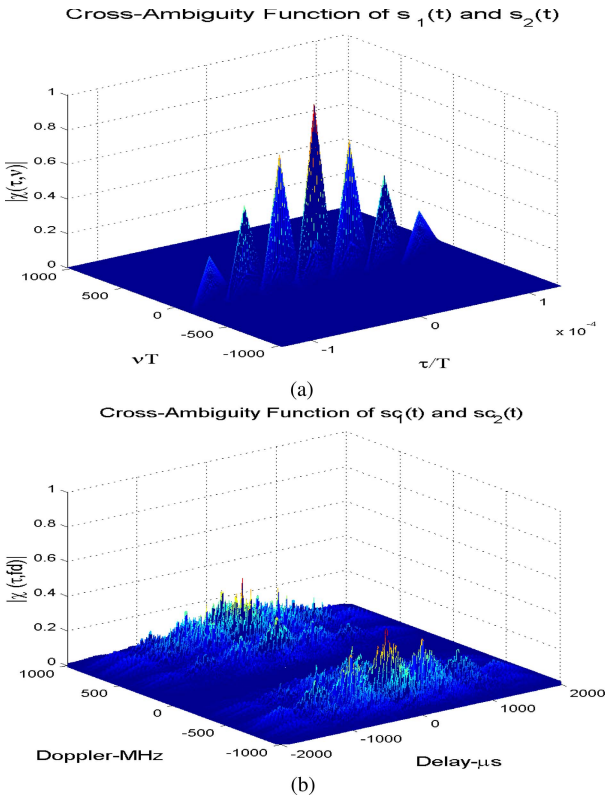

Fig. 7. Auto-ambiguity function results. (a) $s_1(t)$ and $s_2(t)$. (b) $sc_1(t)$ and $sc_2(t)$.

As expected, the auto-ambiguity function of $sc_1(t)$ takes similar shape of $s_1(t)$. Figure 7 gives the cross-ambiguity function (CAF) between $sc_1(t)$ and $sc_2(t)$ with Walsh-Hadamard code of length 64 as well as the CAF of $s_1(t)$ and $s_2(t)$. It can be noticed that the cross-ambiguity peak of $sc_1(t)$ and $sc_2(t)$ is 0.4196, whereas the cross-ambiguity function of $s_1(t)$ and $s_2(t)$ takes similar shape with the auto-ambiguity function of $s_1(t)$. It is clear that our method significantly improves the waveform orthogonality performance, which is beneficial for separating closely spaced targets.

B. SSCTOC Waveforms and SSCOC Waveforms Comparison

Furthermore, we compare our method with the SSCTOC scheme, which uses direct sequence spread spectrum technique to modulate the basic two-OFDM chirp waveform.

The basic two-OFDM scheme generates two waveforms:

$$x_1(t) = \frac{1}{\sqrt{2}}\left\{s(t)\text{rect}\left[\frac{t}{T_p}\right] + s(t-T_p)\text{rect}\left[\frac{t-T_p}{T_p}\right]\right\} \quad (18)$$

$$x_2(t) = x_1(t)\exp\left(j\pi\frac{t}{T_p}\right). \quad (19)$$

We take $x_1(t)$, $x_2(t)$, $s_1(t)$ and $s_2(t)$ as an example to compare their performance. Walsh-Hadamard code is used in the simulations. Table V compares the maximal CAF, namely $\max\{CAF\}$. It is clear that our SSCOC waveforms offer better CAF properties than SSCTOC waveforms.

TABLE V
CAF RESPONSE COMPARISON BETWEEN SSCOC WAVEFORMS AND SSCTOC WAVEFORMS

code type	code length	signal type	$\max\{CAF\}$
Walsh	4	SSCTOC	0.7445
Walsh	4	SSCOC	0.7234
Walsh	8	SSCTOC	0.7092
Walsh	8	SSCOC	0.6649
Walsh	16	SSCTOC	0.5909
Walsh	16	SSCOC	0.5551
Walsh	32	SSCTOC	0.4896
Walsh	32	SSCOC	0.4887
Walsh	128	SSCTOC	0.3679
Walsh	128	SSCOC	0.3649

TABLE VI
CAF RESPONSE COMPARISON BETWEEN SSCL WAVEFORMS AND SSCOC WAVEFORMS

code type	code length	signal type	$\max\{CAF\}$
-	1	SSCL	0.6055
-	1	SSCOC	0.9988
Walsh	8	SSCL	0.4066
Walsh	8	SSCOC	0.6649
Walsh	64	SSCL	0.2466
Walsh	64	SSCOC	0.4196
Walsh	128	SSCL	0.2019
Walsh	128	SSCOC	0.2633

C. SSCL Waveforms and SSCOC Waveforms Comparison

Majumder *et al.* [11] propose a direct sequence spread spectrum modulated linearly frequency modulation (SSCL) signals. Table VI shows the comparative performance between SSCL waveforms and SSCOC waveforms. Without loss of generality, Walsh-Hadamard code is used in the simulation.

Note that the signals are not coded by the spread spectrum sequences. It is obvious that the SSCL waveform yields better CAF response than the SSCOC waveform. A larger starting frequency difference offers a better suppression performance of the cross-correlation components [17].

VI. Conclusion

In this paper, a method is proposed to design SSCOC waveforms by combining the OFDM chirp scheme and direct sequence spread spectrum technique. Simulation results show that the proposed method can maintain good orthogonality in the radar returns. It can be summarized as: 1) The GOLD sequence is the best suitable code to reduce the cross-ambiguity peak. 2) The bandwidth and duration have little influence on the cross-ambiguity response. 3) The SSCOC waveform scheme has a better cross-correlation suppression performance than the basic OFDM chirp waveform scheme. 4) This waveform inherits Doppler tolerant of the OFDM chirp waveform and shows good cross-range and cross-velocity ambiguity properties. 5) The SSCOC waveforms offers better CAF response than the SSCTOC waveform and basic OFDM chirp waveform while poorer CAF response than SSCL waveforms. This paper focuses on waveforms diversity design, in subsequent work, we plan to further investigate the applications of the designed waveforms in a noisy environment.

References

[1] D. Cerutti-Maori, I. Sikaneta, J. Klare, and C. H. Gierull, "MIMO SAR processing for multichannel high-resolution wide-swath radars," *IEEE Trans. Geosci. Remote Sens.*, vol. 52, no. 8, pp. 5034–5055, Aug. 2014.

[2] W.-Q. Wang, "MIMO SAR imaging: Potential and challenges," *IEEE Aerosp. Electron. Syst. Mag.*, vol. 28, no. 8, pp. 18–23, Aug. 2013.

[3] D. Tarchi, F. Oliveri, and P. F. Sammartino, "MIMO radar and ground-based SAR imaging systems: Equivalent approaches for remote sensing," *IEEE Trans. Geosci. Remote Sens.*, vol. 51, no. 1, pp. 425–435, Jan. 2013.

[4] W.-Q. Wang, "Large-area remote sensing in high-altitude high-speed platform using MIMO SAR," *IEEE J. Sel. Topics Appl. Earth Observ. Remote Sens.*, vol. 6, no. 5, pp. 2146–2158, Oct. 2013.

[5] R. Calderbank, S. D. Howard, and B. Moran, "Waveform diversity in radar signal processing," *IEEE Signal Process. Mag.*, vol. 26, no. 1, pp. 32–41, Jan. 2009.

[6] S. R. J. Axelsson, "Suppressed ambiguity in range by phase-coded waveforms," in *Proc. IEEE Int. Geosci. Remote Sensing Symp. (IGARSS)*, vol. 5. Jul. 2001, pp. 2006–2009.

[7] C.-F. Chang and M. R. Bell, "Frequency-coded waveforms for enhanced delay-Doppler resolution," *IEEE Trans. Inf. Theory*, vol. 49, no. 11, pp. 2960–2971, Nov. 2003.

[8] S. D. Howard, A. R. Calderbank, and W. Moran, "A simple signal processing architecture for instantaneous radar polarimetry," *IEEE Trans. Inf. Theory*, vol. 53, no. 4, pp. 1282–1289, Apr. 2007.

[9] I. Gladkova, "Analysis of stepped-frequency pulse train design," *IEEE Trans. Aerosp. Electron. Syst.*, vol. 45, no. 4, pp. 1251–1261, Oct. 2009.

[10] B. Friedlander, "On the relationship between MIMO and SIMO radars," *IEEE Trans. Signal Process.*, vol. 57, no. 1, pp. 394–398, Jan. 2009.

[11] U. K. Majumder, M. R. Bell, and M. Rangaswamy, "A novel approach for designing diversity radar waveforms that are orthogonal on both transmit and receive," in *Proc. IEEE Radar Conf. (RADAR)*, Ottawa, ON, Canada, Apr. 2013, pp. 1–6.

[12] J.-H. Kim, M. Younis, A. Moreira, and W. Wiesbeck, "A novel OFDM chirp waveform scheme for use of multiple transmitters in SAR," *IEEE Trans. Geosci. Remote Sens.*, vol. 10, no. 3, pp. 568–572, May 2013.

[13] N. Levanon, "Multifrequency complementary phase-coded radar signal," *IEE Proc.-Radar, Sonar Navigat.*, vol. 147, no. 6, pp. 276–284, Dec. 2000.

[14] D. R. Fuhrmann, J. P. Browning, and M. Rangaswamy, "Signaling strategies for the hybrid MIMO phased-array radar," *IEEE J. Sel. Topics Signal Process.*, vol. 4, no. 1, pp. 66–78, Feb. 2010.

[15] D. Garmatyuk, J. Schuerger, K. Kauffman, and S. Spalding, "Wideband OFDM system for radar and communications," in *Proc. IEEE Radar Conf.*, Pasadena, CA, USA, May 2009, pp. 1–6.

[16] W.-Q. Wang, *Multi-Antenna Synthetic Aperture Radar*. New York, NY, USA: CRC Press, May 2013.

[17] W.-Q. Wang, "Space–time coding MIMO-OFDM SAR for high-resolution imaging," *IEEE Trans. Geosci. Remote Sens.*, vol. 49, no. 8, pp. 3094–3104, Aug. 2011.

[18] G. Krieger *et al.*, "MIMO-SAR and the orthogonality confusion," in *Proc. IEEE Int. Geosci. Remote Sens. Symp. (IGARSS)*, Munich, Germany, Jul. 2012, pp. 1533–1536.

[19] H. Yan, G. Shen, R. Zetik, O. Hirsch, and R. S. Thoma, "Ultra-wideband MIMO ambiguity function and its factorability," *IEEE Trans. Geosci. Remote Sens.*, vol. 51, no. 1, pp. 504–519, Jan. 2013.

[20] J. C. Curlander and R. N. McDonough, *Synthetic Aperture Radar: Systems and Signal Processing*. New York, NY, USA: Wiley, 1991.

[21] N. Levanon and E. Mozeson, *Radar Signals*. Chichester, U.K.: Wiley, 2004.

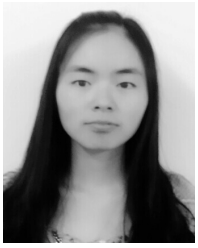

Sheng-Juan Cheng received the B.E. degree in electronic information science and technology from Three Gorges University, Hubei, China, in 2012, and the M.E. degree in information and communication engineering from the University of Electronic Science and Technology of China, Chengdu, China, in 2015. She is currently with Huawei Technologies Company, Ltd. Her interests include signal processing in communication and radar applications.

Wen-Qin Wang (M'08) received the B.S. degree in electrical engineering from Shandong University, Shandong, China, in 2002, and the M.E. and Ph.D. degrees in information and communication engineering from the University of Electronic Science and Technology of China (UESTC), Chengdu, China, in 2005 and 2010, respectively.

He was with the National Key Laboratory of Microwave Imaging Technology, Chinese Academy of Sciences, Beijing, China, from 2005 to 2007. Since 2007, he has been with the School of Communication and Information Engineering, UESTC, where he is currently a Professor. From 2011 to 2012, he was a Visiting Scholar with the Stevens Institute of Technology, NJ, USA. From 2012 to 2013, he was a Hong Kong Scholar with the City University of Hong Kong, Hong Kong. He has authored two books published by Springer and CRC Press, respectively. His research interests include communication and radar signal processing, and novel radar imaging techniques. He holds also a Marie Curie International Incoming Fellow position with Imperial College London, U.K.

Prof. Wang was a recipient of Marie Curie Fellow and Hong Kong Scholar. He is also the Editorial Board Member of four international journals.

Huai-Zong Shao received the M.S. degree in electrical engineering from Sichuan University, Chengdu, China, in 1998, and the Ph.D. degree in information and communication engineering from the University of Electronic Science and Technology of China (UESTC), Chengdu, China, in 2003. Since 2003, he has been with the School of Communication and Information Engineering, UESTC, where he is currently an Associate Professor. His research interests include communication and radar signal processing.